JOURNAL OF VIROLOGY, Oct. 2002, p. 9952–9961 Vol. 76, No. 19
0022-538X/02/$04.00+0 DOI: 10.1128/JVI.76.19.9952–9961.2002


# Inhibitory Activity of Synthetic Peptide Antibiotics on Feline Immunodeficiency Virus Infectivity In Vitro

Jia Ma,[1]* Suzanne Kennedy-Stoskopf,[1] Jesse M. Jaynes,[2] Linda M. Thurmond,[3] and Wayne A. Tompkins[1]

*Department of Microbiology, Pathology, and Parasitology, North Carolina State University, Raleigh, North Carolina[1]; Demegen, Inc., Pittsburgh, Pennsylvania[2]; and Glaxo SmithKline Inc., Research Triangle Park, North Carolina[3]*

Received 25 January 2002/Accepted 14 June 2002

**Natural peptide antibiotics are part of host innate immunity against a wide range of microbes, including some viruses. Synthetic peptides modeled after natural peptide antibiotics interfere with microbial membranes and are termed peptidyl membrane-interactive molecules (peptidyl-MIM [Demegen Inc, Pittsburgh, Pa.]). Sixteen peptidyl-MIM candidates were tested for activity against feline immunodeficiency virus (FIV) on infected CrFK cells. Three of them (D4E1, DC1, and D1D6) showed potent anti-FIV activity in chronically infected CrFK cells as measured by decreased reverse transcriptase (RT) activity, having 50% inhibitory concentrations of 0.46, 0.75, and 0.94 μM, respectively, which were approximately 10 times lower than their direct cytotoxic concentrations. Treatment of chronically infected CrFK cells with 2 μM D4E1 for 3 days completely reversed virus-induced cytopathic effect. Immunofluorescence revealed reduced p26 staining in these cells. Treatment of chronically infected CrFK cells with 2 μM D4E1 suppressed virus production (~50%) for up to 7 days, The virions from the D4E1-treated culture had impaired infectivity, as measured by the 50% tissue culture infectious dose and nested PCR analysis of proviral DNA. However, these noninfectious virions were able to bind and internalize, suggesting a defect at some postentry step. After chronically infected CrFK cells were treated with D4E1 for 24 h, increased cell-associated mature p26 Gag and decreased extracellular virus-associated p26 Gag were observed by Western blot analysis, suggesting that virus assembly and/or release may be blocked by D4E1 treatment, whereas virus binding, penetration, RNA synthesis, and protein synthesis appear to be unaffected. Synthetic peptide antibiotics may be useful tools in the search for antiviral drugs having a wide therapeutic window for host cells.**

Significant progress has been made in the treatment of human immunodeficiency virus (HIV) infection, but we are still far from the end of the battle against this disease. Current therapy consists of complex regimens of nucleoside analogs, nonnucleoside reverse transcriptase inhibitors, and viral protease inhibitors aimed at specific steps of the HIV replication cycle. These drugs target with high specificity, yet rapid virus turnover in HIV infection may result in the emergence of resistant mutants and subsequent treatment failure (7, 36). The search continues for new drugs having lower toxicity that attack novel HIV targets or different components of the HIV replication cycle or simply provide more choice for combinatory therapy.

Peptide antibiotics (also known as antimicrobial peptides or natural antibiotics) can be isolated from a variety of organisms, including bacteria, plants, insects, invertebrates, and vertebrates. These peptides are among the main effector molecules in host innate immunity and act on a variety of tumor cells as well as a broad spectrum of microbes such as bacteria, fungi, protozoa, and enveloped viruses. Features common to all the peptide antibiotics are small size (12 to 100 amino acid residues), polycationic charge, and amphipathic structure having associated α-helices or β-pleated sheets (reviewed in reference 3). The currently proposed antimicrobial mechanism of this class of agent is direct electrostatic interaction with negatively charged microbial cell membranes, followed by physical disruption (3, 19, 32).

The natural peptide antibiotics have been proposed for use against infectious diseases as an alternative for conventional antibiotics due to their apparently minimal tendency to induce microbial resistance (12, 13). Anti-HIV activities have been described for several peptide antibiotics, such as melittin and cecropin (both α-helix forms of peptides), from insects (45, 46), and tachyplesins (29) and protegrins (42) (small β-sheet peptides), found in the blood cells of horseshoe crabs and pigs, respectively. Peptides modeled on these natural peptide antibiotics have been synthesized to facilitate the study of structure-function relationships and the mechanism of action of antimicrobial activity (16). These synthetic peptides are termed peptidyl membrane-interactive molecules (peptidyl-MIMs). Preliminary testing of some of these peptidyl-MIMs has shown antimicrobial activity greater than that of their natural analogs (16).

Critical to evaluating the in vivo efficacy of peptidyl-MIMs as therapies for AIDS is an animal model that closely resembles HIV in natural history and pathogenesis. Feline immunodeficiency virus (FIV) is a lentivirus of the cat that closely parallels the natural history, pathogenesis, and development of immunodeficiency and clinical diseases seen in HIV infection (10, 35, 44). The morphology, protein composition, and genomic organization of FIV are similar to those of other lentiviruses,

* Corresponding author. Present address: Glaxo SmithKline, EH.A2217C.2G, 5 Moore Dr., Research Triangle Park, NC 27709. Phone: (919) 483-8440. Fax: (919) 315-6003. E-mail: jzm83081@gsk.com.

TABLE 1. Synthetic peptide antibiotics tested for antiviral (FIV) activity and their structural characteristics

| Peptidyl-MIM | Amino acid sequence | Secondary structure |
|---|---|---|
| D4E1 | FKLRAKIKVRLRAKIKL | β-Pleated sheets |
| DC1 | FAVAVKAVAVKAVAVKAVKKAVKKVKKAVKKAVKKKK | α-Helix |
| D1D6 | FLAAARIAKRVAKKARKLAKRAARKRK | α-Helix |
| D4C3 | FRFKIKFRLKFRFKARFKFRAKFRA | β-Pleated sheets |
| D5C1 | KRKRAVKRVGRRLKKLARKIARLGVAKLAGLRAVKLF | α-Helix |
| D5F | FAVGLRAIKRALKKLRRGVRKVAKDL | α-Helix |
| D2B15 | GAKKGAKKGKKGAKKGAKGAGAKGAGAFKKKK | α-Helix |
| D2A3 | KKKKFVKKVAKKVKKVAKKVAKVAVAV | α-Helix |
| D2A21 | FAKKFAKKFKKFAKKFAKFAFAF | α-Helix |
| D1A22 | FLFAFRIFKRVFKKFRKLFKRAF | α-Helix |
| D5C | KRKRAVKRVGRRLKKKLARKIARLGVAF | α-Helix |
| D3A15 | KRKRFAKKFLRFLRKVIRFLKRFIRRF | α-Helix |
| D1D2 | FAIAIKAIKKAIKKIKKAIKKAI | α-Helix |
| DP1 | FALALKALKKALKKLKKALKKAL | α-Helix |
| D4B | FKVKAKVKAKVKAKVKAKKKK | β-Pleated sheets |
| D5D | AVKRVGRRLKKLARKIARLGVAF | α-Helix |

including HIV. Although FIV's overall genomic organization is more closely related to that of nonprimate lentiviruses, the biology of FIV resembles that of HIV, as it is highly lymphotropic and causes an immunodeficiency syndrome. Molecular cloning and characterization of the gene and gene products encoded by FIV make it amenable to molecular manipulations for detailed studies of the lentivirus life cycle and development of intervention strategies (30, 39).

In this study, we took advantage of the FIV infection model to evaluate the potential in vitro antiviral activity, cell toxicity, and mechanism of action of peptidyl-MIM synthetic peptide antibiotics.

## MATERIALS AND METHODS

**Cells.** Uninfected Crandell feline kidney (CrFK) cells and CrFK cells persistently infected with either the Black or Petaluma isolate of FIV were maintained in Dulbecco's modified Eagle's medium (DMEM) supplemented with 10% heat-inactivated fetal bovine serum (FBS), 2 mM L-glutamine, 100 U of penicillin per ml, 100 μg of streptomycin per ml, 15 mM HEPES, and 0.075% $NaHCO_3$. Approximately 80% of the cells in the chronically infected CrFK cell culture expressed FIV proteins when measured by immunofluorescence.

FCD4-E, an interleukin-2 (IL-2)-dependent feline $CD4^+$ lymphocyte cell line established in our laboratory (31), was used to assay infectious FIV. FCD4-E cells were maintained in RPMI medium supplemented with 10% FBS, 100 U of penicillin per ml, 100 μg of streptomycin per ml, 2 mM L-glutamine, 15 mM HEPES, 2 mM sodium pyruvate, $5 \times 10^{-5}$ M 2-β-mercaptoethanol, and 100 U of recombinant human IL-2 (rhIL-2; Biological Resource Branch, National Cancer Institute, Frederick, Md.) per ml.

**FIV isolates.** Two FIV isolates, FIV-Black (obtained from J. Black, American Bioresearch, Inc., Milton, Tenn.) and FIV-Petaluma (obtained from the American Type Culture Collection, Manassas, Va.), were used in the experiments. These two virus isolates were distinguishable by cellular cytopathic effects. FIV-Black virus-infected CrFK cells showed normal cell morphology. In contrast, Petaluma-infected cells form syncytia and show cell rounding, formation of cytoplasmic granules, and slower growth. Both isolates of FIV were maintained in chronically infected CrFK cells.

**Peptidyl-MIM compound candidates.** A total of 16 peptidyl-MIM candidates were provided by Demegen, Inc. (Pittsburgh, Pa.). They were D4E1, DC1, D1D6, D4C3, D5C1, D5F, D2B15, D2A3, D2A21, D1A22, D5C, D3A15, D1D2, DP1, D4B, and D5D (Table 1). Peptides were dissolved in double-distilled $H_2O$ at a 1 mM concentration, aliquoted, and stored at −80°C. For assay, peptidyl-MIMs were thawed on the day of use and diluted in culture medium to the indicated final concentration.

**Antibodies.** Monoclonal antibody specific for FIV Gag protein (clone 51G11.1) was a gift from E. A. Hoover (Colorado State University, Fort Collins). Fluorescein isothiocyanate (FITC)-conjugated goat anti-mouse immunoglobulin G (IgG) and peroxidase-labeled goat anti-cat IgG were purchased from Kirkegaard-Perry Laboratories (Gaithersburg, Md.). Serum from an FIV-infected specific-pathogen-free cat (KJ6, experimentally infected with the $NCSU_1$ strain of FIV) was used to detect FIV antigens for Western blot analysis. The serum was preabsorbed overnight at 4°C with uninfected CrFK cells, and the supernatant containing anti-FIV antibody was collected after centrifugation.

**Determination of antiviral and cytotoxic effect of peptidyl-MIMs.** Chronically FIV (Black or Petaluma)-infected CrFK cells were seeded into the wells of 96-well plates at $10^4$ cells in 100 μl of assay medium (DMEM with only 5% FBS but otherwise containing the same supplements as culture medium). To triplicate wells, 100 μl of medium containing serially diluted peptidyl-MIMs was added. After a 24-h incubation at 37°C in 7% $CO_2$, supernatants were collected for reverse transcriptase (RT) assay or p26 determination, and cells were assayed for peptidyl-MIM cytotoxicity. Uninfected CrFK cells were similarly treated to measure the cytotoxicity of peptidyl-MIMs for normal cells. For testing long-term effects of peptide treatment, supernatants were also collected at 3, 5, and 7 days. Data obtained from RT assays, p26 enzyme-linked immunosorbent assay (ELISA), and MTT [3-(4,5-dimethylthiozol-2-yl)-2,5-diphenyl tetrazolium bromide] assays were converted into relative values by calculating the percentage obtained from peptidyl-MIM-treated samples relative to untreated control samples. The 50% inhibitory concentration ($IC_{50}$) and 50% toxic concentration ($TC_{50}$) were calculated by linear regression analysis.

**RT assay.** FIV RT activity in the samples was measured in a standard enzyme assay (31). Briefly, 10 μl of a test sample was added to 50 μl of RT reaction mix {50 mM Tris-HCl (pH 8.0), 5 mM $MgCl_2$, 7.5 mM KCl, 2 mM dithiothreitol, 0.5 μg of poly(rA):oligo$(dT)_{15}$ per ml, 0.05% Nonidet P-40, and 0.5 μCi of [α-$^{32}$P]TTP} and incubated in a 37°C water bath for 2 h. Products (10 μl) of each reaction were spotted on DE-81 ion-exchange paper (Whatman) in triplicate and allowed to dry for 30 min. Papers were washed with 2× SSC (1× SSC is 0.15 M NaCl plus 0.015 M sodium citrate) four times for 5 min each and allowed to dry for another 30 min. Dried filters were placed into dry scintillation tubes, and radioactivity was counted.

**Cell cytotoxicity assay.** The MTT cytotoxicity assay was performed as previously described (26) with minor modifications. Briefly, medium was removed from peptidyl-MIM-treated and untreated cell culture wells, and 150 μl of fresh medium was added per well. MTT (Sigma) was dissolved in phosphate-buffered saline (PBS) (5 mg/ml), and 25 μl was added to each well. The plate was incubated at 37°C in 7% $CO_2$ for 4 h, then all supernatants were removed, and 100 μl of 0.1 N HCl in isopropanol was added to each well. After 30 min of incubation, 100 μl of distilled water was added to each well, and the plate was read at 570- and 630-nm dual wavelengths in a kinetic microplate reader (Molecular Devices Corporation, Sunnyvale, Calif.). The wavelength-corrected optical density is proportional to the number of viable cells able to reduce the MTT to insoluble formazan dye. Untreated wells were used as the positive control for 100% viability.

**Chamber slide cell culture.** Two-well glass slides (Lab-Tek chamber slides; Nalge Nunc International) were seeded with $10^5$ cells of uninfected or chronically FIV-Petaluma-infected CrFK cells. D4E1 peptidyl-MIM was diluted in medium at various concentrations and added to each well to a total volume of 1 ml. Cells were cultured at 37°C in 7% $CO_2$ for 3 days. The morphology of and cytopathic effect on the cells in untreated and treated wells were observed under

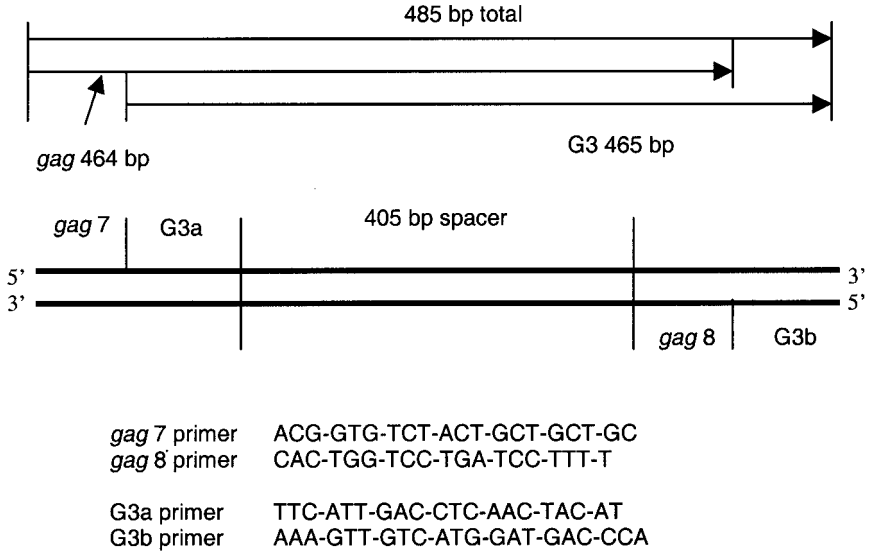


FIG. 1. RT-qcPCR strategy for amplification of FIV Gag protein. The competitive fragment was constructed starting with the *gag* 7 and G3a primers, then a 405-bp spacer (segment of the feline herpes virus thymidine kinase gene), followed by the *gag* 8 and G3b primers. The full-length fragment is 485 bp. The *gag* 7 and *gag* 8 primer pair amplify a 464-bp product, and the G3a and G3b primer pair amplify a 465-bp product.

a phase-contrast microscope. The slides then were disassembled and rinsed with PBS. They were either stained immediately with Leukostat fixative solution (Fisher Scientific) for light microscopy or fixed in methanol-acetone (1:1) at −20°C for 8 min and stored at −20°C for immunofluorescence staining.

**Immunofluorescence stain of FIV protein.** Slides stored at −20°C were allowed to thaw at room temperature for 5 min. Slides were blocked with 150 μl of 5% bovine serum albumin for 30 min, washed three times with PBS, and incubated for 30 min with primary antibody (anti-FIV Gag) diluted to 30 μg/ml in PBS containing 5% bovine serum albumin. Primary antibody was omitted from one slide each of infected and uninfected cells to check for nonspecific binding. After washing slides three times with PBS, goat anti-mouse IgG-FITC (diluted to 2.5 μg/ml in PBS with 5% bovine serum albumin) was added, and the slides were incubated for another 30 min in the dark. Slides were washed three times with PBS, then blotted, and covered with a glass coverslip after applying a drop of glycerol-PBS. An epifluorescence microscope equipped for photomicroscopy was used for viewing.

**Assay for virus antigen and infectious FIV ($TCID_{50}$).** FIV p26 antigen capture ELISA was performed with either the low-range ELISA kit (Idexx Corp., Portland, Maine) or high-protein-range ELISA method (North Carolina State University), depending on the relative p26 concentration. The 50% tissue culture infectious dose ($TCID_{50}$) assay for infectious FIV was performed on FCD4-E cells (22). Cells suspended in 100 μl of culture medium containing 200 U of rhIL-2 per ml were seeded at $10^5$ cells with a viability of ≥80% into 96-well plates. Supernatants from chronically Petaluma-infected CrFK cells, with or without peptidyl-MIM treatment for 7 days, were serially diluted 10-fold in medium (without rhIL-2), and 100 μl was added to cells in five replicate wells. Cells were cultured for 21 days at 37°C in 5% $CO_2$, and supernatants were assayed for p26 by ELISA (Idexx Corp., Portland, Maine). The $TCID_{50}$ was calculated by the Reed-Muench method (14).

**Virus binding and entry assay.** Virus binding and entry assays were performed according to the method of de Parseval et al. (9) with minor modifications. To assay for virus binding, the monolayer of CrFK cells in a 25-$cm^2$ flask ($3 \times 10^6$ cells cultured overnight) was cooled on ice for 30 min and infected with 100 μl of FIV-Petaluma with or without 2 μM D4E1. Cells were incubated on ice for 1 h and washed five times in ice-cold PBS to remove unbound virus. The monolayer was then directly lysed by adding RLT lysis buffer (Qiagen) to the flask. For internalization studies, cells were infected with 100 μl of FIV-Petaluma at 37°C in 7% $CO_2$ for 1 h and washed five times with PBS, and then 1 ml of trypsin-EDTA (0.25%) was added for 10 min at 37°C and 7% $CO_2$. Cells were then washed in ice-cold assay medium and PBS one time each by centrifugation for 5 min at 280 × *g*, followed by lysis in RLT buffer. The total cell-associated viral RNA was extracted by using an RNeasy RNA purification kit (Qiagen) and quantitated by RT-PCR and RT–quantitative-competitive PCR (qcPCR).

To test whether virions produced in the presence of D4E1 are infectious, two different volumes of supernatant (100 and 45 μl, to normalize virions based on p26 in the supernatant) from D4E1-treated and untreated cultures were added to monolayers of CrFK cells and assayed for binding and internalization as described above.

**Determination of FIV RNA levels in chronically infected CrFK cells.** CrFK cells chronically infected with FIV-Petaluma were diluted to $4 \times 10^5$ cells in 1.9 ml of assay medium (5% FBS) and added to the wells of a six-well plate (Costar). D4E1 or medium alone was added at 100 μl per well at a final concentration of 2 μM, and the plates were incubated for 24 h. Supernatant was removed from each well, and the plate was washed three times with PBS. Tri-Reagent was added to each well to extract total RNA from the cell monolayers.

The RT-qcPCR was performed as described by Rottman et al. (38) with minor modifications. The primers for detection and quantification of FIV RNA were selected from the published sequence for FIV-Petaluma (41). Primers *gag* 7 and *gag* 8 amplify an 834-bp sequence of the *gag* open reading frame. The primers for glyceraldehyde-3-phosphate dehydrogenase (G3PDH, internal control) were selected from consensus sequences from other mammalian species obtained from the GenBank database (38) (Fig. 1).

PCR was used to amplify a reaction series containing equal amounts of cDNA in the presence of serial fivefold dilutions (six reactions/series) of a known amount of competitive DNA fragment (25 pg/ml down to $8 \times 10^{-3}$ pg/ml [Fig. 1]). The 485-bp competitive DNA fragment consisted of both the upstream and downstream primer sites for *gag* and G3PDH separated by a 405-bp DNA spacer. Amplification of the fragment with each primer set yields products of 464 and 465 bp that are different from the length of the cDNA products (Fig. 1). The PCR master mix (containing cDNA to be tested) was prepared, and 20 μl was added to 96-well V-bottomed PCR plates (Thermowell) which contained 5 μl of the appropriate serial competitor dilutions. The plate was placed in the thermal cycler and initially heated to 94°C for 1 min, followed by 40 cycles of 94°C for 30 s, 57°C for 90 s, and 72°C for 120 s, with a final 10 min at 72°C.

The amplified competitive fragment and cDNA PCR products were separated by electrophoresis on a Tris-acetate-EDTA 2% agarose gel, visualized with ethidium bromide and a UV transilluminator, and photographed with a Polaroid camera. The image was scanned into Adobe Photoshop and analyzed with a National Institutes of Health image software program to measure the fluorescence of the target and competitor bands in each lane. A fluorescence ratio was calculated to compensate for differences in fluorescence intensity due to molecular weight. The log of the corrected fluorescence ratio was plotted against the log of the number of copies of competitor in the sample, yielding the number of copies of target at the X intercept (molecular equivalence). The amount of *gag* RNA was presented as a ratio of *gag* to G3PDH to allow quantitative comparison between samples.

**Western blot analysis of intracellular and extracellular FIV proteins.** Uninfected or chronically infected (FIV-Petaluma) CrFK cells were seeded into 75-cm$^2$ culture flasks (Costar) at $5 \times 10^6$ cells per 10 ml of assay medium (DMEM with 5% FBS). D4E1 (2 μM final concentration) was added to the flasks. After culturing cells for 24 h, supernatants were collected for extracellular viral protein analysis; cells were trypsinized, washed, and counted prior to analysis of cell-associated virus proteins.

Supernatants (about 9 ml) were centrifuged at 400 × *g* for 5 min at 22°C to eliminate cell debris. Then 7 ml of supernatant (2 ml was reserved for the p26 ELISA and RT assays) was ultracentrifuged at 100,000 × *g* for 30 min at 4°C. Supernatant was discarded, and 100 μl of lysis buffer (50 mM Tris HCl [pH 8.3] containing 20 mM dithiothreitol and 0.25% Triton X-100) was added to the pellet. Samples were transferred to a 0.5-ml microcentrifuge tube and stored at −20°C for later Western blot analysis.

Trypsinized cell suspensions were centrifuged, and the supernatant was decanted. The cell pellets were resuspended in 1 ml of PBS and transferred to 1.5-ml microcentrifuge tubes. Tubes were centrifuged at 5,000 rpm for 5 min at 4°C. Supernatants were discarded, and 100 μl of ice-cold homogenizing buffer (0.2 mM EGTA, 0.2 mM EDTA, 2 mM HEPES, 0.5% Triton X-100, 20 μg of leupeptin per ml, and 1 mM phenylmethylsulfonyl fluoride) was added to approximately $5 \times 10^6$ cells. The cell pellets were resuspended by trituration and sonicated on ice. The lysates were held on ice for 30 min, then transferred to ultracentrifuge tubes, and spun at 100,000 × *g* for 1 h at 4°C. The supernatant was collected and stored at −20°C for later Western blot analysis.

Western blot analysis was performed by the method of Johnson et al. (17) with minor modification. Briefly, 5× sample buffer (0.3125 M Tris-HCl [pH 6.8] containing 50% glycerol, 10% sodium dodecyl sulfate [SDS], and 0.01% bromophenol blue) was warmed in a 60°C water bath, and 2-mercaptoethanol was added at a final concentration of 5%. Cellular protein was diluted to 15 μg (as determined by the BCA protein assay; Pierce Chemical Co.) in sample buffer in a total volume of 30 μl. Samples were denatured in boiling water for 5 min and cooled on ice, and 25 μl of sample per lane was loaded in the gel. Virus lysates were mixed with sample buffer (usually 2.5 μl of virus lysate in a total 25-μl volume per lane) and loaded on the gel. Sodium dodecyl sulfate-polyacrylamide gel electrophoresis (SDS-PAGE) was performed with a Tris-glycine precast gradient (4 to 20%) gel (Novex, San Diego, Calif.) at 125 V for 90 min. The gel was electroblotted to nitrocellulose membranes, immunostained with FIV$^+$ cat serum at a 1:1,000 dilution followed by peroxidase-labeled goat anti-cat IgG at 0.2 μg/ml, and revealed by enhanced chemiluminescence.

**Nested PCR and limiting-dilution analysis of proviral DNA.** Monolayers of CrFK cells in a 25-cm$^2$ flask ($3 \times 10^6$ cells cultured overnight) were infected for 3 days with either 100 or 45 μl of supernatant (normalized based on p26) from 7-day D4E1-treated or untreated FIV-infected CrFK cultures. The DNA was purified with the QIAamp DNA blood mini kit (Qiagen), serially diluted to an equivalent of $10^5$, $10^4$, $10^3$, and $10^2$ cells, and subjected to nested PCR analysis.

Nested PCR was performed as described by Rogers et al. (37) with minor modifications. Briefly, an FIV *gag* primer pair (Gag 1, 5′-GGGAATGGACAG GGGCGAGAT-3′, and Gag 2, 5′-TTGCTGCACTTGATTCACTGG-3′) amplified a 1,300-bp *gag* fragment. The thermocycler was programmed to 35 cycles of 94°C for 1 min, 58°C for 1 min, and 72°C for 1 min, with a final 2 min at 72°C after initial hot-start activation of 95°C for 15 min. The PCR products were diluted to 1:500, and 1 μl per 25 μl of reaction volume was amplified with a second primer pair (Gag 3, 5′-TTGACCCAAAAATGGTGTCCA-3′, and Gag 5, 5′-GCTGG TGCAAATCTTGCTTC-3′), yielding a 310-bp fragment nested within the first-round *gag* fragment. The thermocycler was programmed to 35 cycles of 94°C for 45 s, 60°C for 30 s, and 72°C for 45 s, with a final 2 min at 72°C after initial hot-start activation of 95°C for 15 min. G3PDH was amplified only in the first PCR run and served as an internal control.

## RESULTS

**Inhibition of RT activity by peptidyl-MIM.** CrFK cells chronically infected with the Petaluma virus strain were cultured in the presence of serial dilutions of the peptidyl-MIM candidates and screened for FIV RT activity and cell viability at 24 h. The data are summarized in Table 2. Three peptidyl-MIM candidates (D4E1, DC1, and D1D6) have fairly low $IC_{50}$ (0.46 μM, 0.75 μM, and 0.94 μM, respectively) and relatively high $TC_{50}$ (5.90 μM, 9.20 μM, and 8.93 μM, respectively) values, with in vitro therapeutic indices ($TC_{50}/IC_{50}$) of 12.83, 12.27, and 9.50, respectively. The comparable cytotoxicity of peptidyl-MIM for FIV-infected and uninfected CrFK cells suggested that their antiviral activity was not due to a selective toxicity to FIV-infected CrFK cells but was related to inhibition of virus replication. Similar results were obtained with FIV-Black viral isolates tested against D4E1, DC1, D1D6, and D5C (a peptidyl-MIM selected for having low potency), and data for both strains are shown in Table 3.

TABLE 2. $IC_{50}$ and $TC_{50}$ of peptidyl-MIM candidates on chronic FIV-Petaluma-infected and uninfected CrFK cells[a]

| Peptidyl-MIM candidate | $IC_{50}$ (μM) | $TC_{50}$ (μM) | In vitro therapeutic index |
|---|---|---|---|
| D4E1 | 0.46 | 5.90 | 12.83 |
| DC1 | 0.75 | 9.20 | 12.27 |
| D1D6 | 0.94 | 8.93 | 9.50 |
| 4C3 | 1.32 | 3.81 | 2.89 |
| 5F | 5.47 | 8.73 | 1.60 |
| 5C1 | 3.38 | 5.26 | 1.56 |
| D2B15 | 4.07 | 6.19 | 1.52 |
| D2A21 | 3.05 | 3.43 | 1.12 |
| 2A3 | 3.00 | 3.24 | 1.08 |
| D1A22 | 10.51 | 10.79 | 1.03 |
| D5C | 7.82 | 7.48 | 0.96 |
| 3A15 | 3.69 | 3.28 | 0.89 |
| DP1 | 7.07 | 5.17 | 0.73 |
| D1D2 | 8.71 | 5.87 | 0.67 |
| D4B | 2.85 | 0.92 | 0.32 |
| 5D | 3.37 | NA | NA |

[a] Chronically infected CrFK cells were cultured with dilutions of peptidyl-MIM candidates as described in Materials and Method for 24 h. Values were calculated by plotting relative values of RT activity or cell toxicity against peptidyl-MIM concentrations modeled by linear regression analysis. Data are the means of triplicate samples. The in vitro therapeutic index was calculated as the $TC_{50}$ of uninfected cells divided by the $IC_{50}$ for each compound. The $TC_{50}$ values of infected cells were not significantly different from those of uninfected cells ($P = 0.250$). NA, not available.

**Alleviation of FIV cytopathic effect and intracellular p26.** Uninfected CrFK cells formed uniform monolayers of spindle-shaped epithelial cells (Fig. 2A), and treatment with peptidyl-MIM D4E1 had little effect (Fig. 2B). Chronically FIV-Petaluma-infected CrFK cells showed significant rounding and

TABLE 3. Effects of peptidyl-MIM candidates on CrFK cells chronically infected with different FIV strains[a]

| FIV strain | Peptidyl-MIM | $IC_{50}$ (μM) | $TC_{50}$ (μM) | In vitro therapeutic index |
|---|---|---|---|---|
| Petaluma | D4E1 | 0.46 | 5.90 | 12.83 |
| | DC1 | 0.75 | 9.20 | 12.27 |
| | D1D6 | 0.94 | 8.93 | 9.50 |
| | D5C | 7.82 | 7.48 | 0.96 |
| Black | D4E1 | 0.43 | 5.90 | 13.72 |
| | DC1 | 0.78 | 9.20 | 11.79 |
| | D1D6 | 1.47 | 8.93 | 6.07 |
| | D5C | 6.84 | 7.48 | 1.09 |

[a] Chronically infected CrFK cells were cultured with dilutions of peptidyl-MIM candidates as described in Materials and Method for 24 h. Values were calculated by plotting relative values of RT activity or cell toxicity against peptidyl-MIM concentrations modeled by linear regression analysis. Data are the means of triplicate samples. The in vitro therapeutic index was calculated as the $TC_{50}$ of uninfected cells divided by the $IC_{50}$ for each compound. The $TC_{50}$ values of infected cells were not significantly different from those of uninfected cells (FIV-Petaluma, $P = 0.184$; FIV-Black, $P = 0.584$).

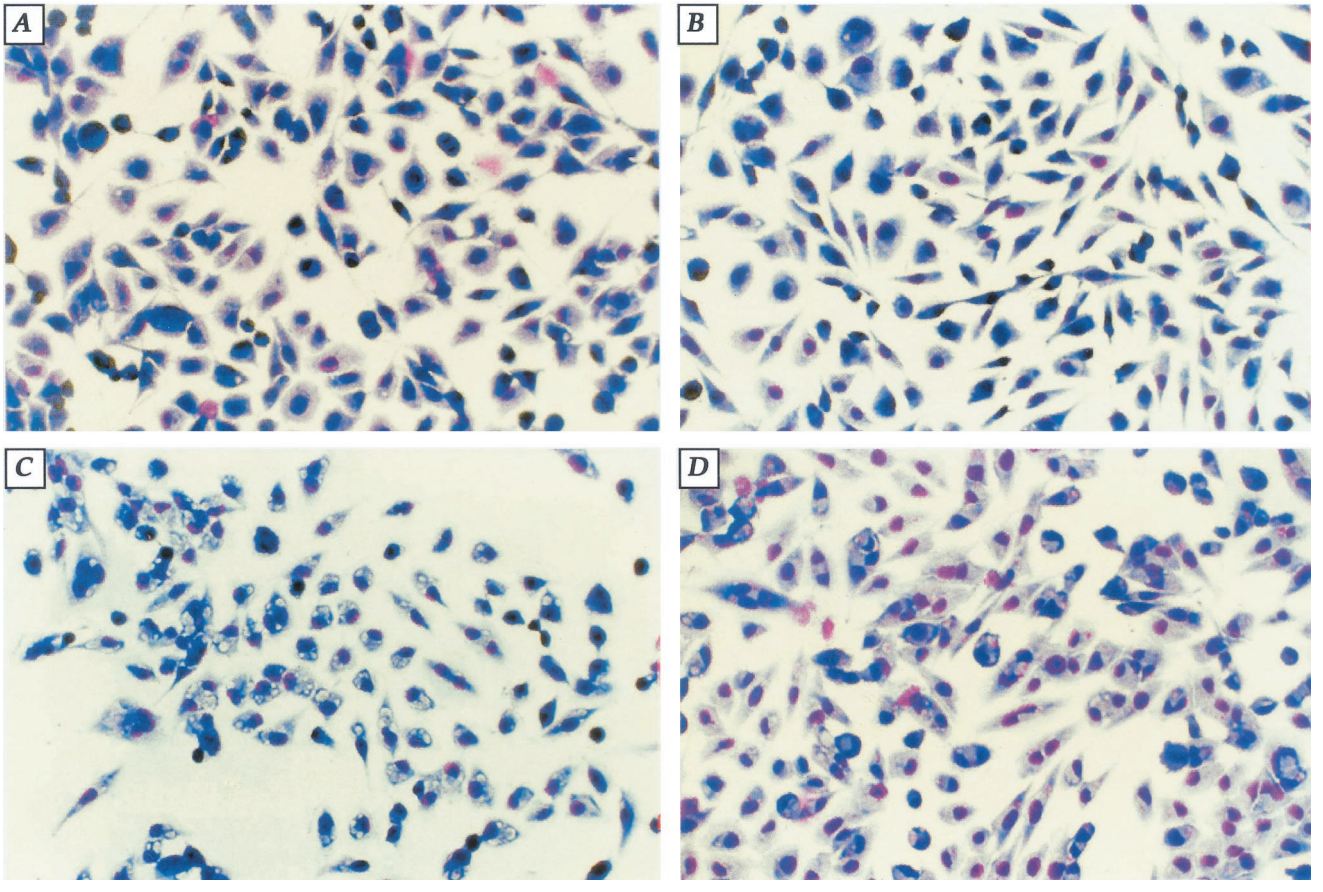


FIG. 2. Cytochemical comparison of cell morphology between uninfected and FIV-Petaluma-infected cells treated with peptidyl-MIM. Uninfected (A and B) and chronically FIV-Petaluma-infected (C and D) CrFK cells were cultured in glass chamber slides and treated with 2 μM D4E1 (B and D) or medium alone (A and C) for 3 days. Slides were reviewed by phase-contrast microscopy, then stained with Leukostat fixative solution, and examined. Magnification, ×200. Normal epithelial cell morphology was evident for uninfected cells and for infected cells treated with peptidyl-MIM D4E1 (A, B, and D). Infected untreated cells showed significant cytopathic effect (C).

detachment of cells, numerous large cytoplasmic vacuoles, and absence of typical spindle morphology (Fig. 2C). Treatment of infected cells with peptidyl-MIM D4E1 resulted in cell growth and morphology indistinguishable from that of uninfected cells during the observation period (Fig. 2D). The effect of D4E1 treatment on the morphology of infected cells was dose dependent (data not shown).

Staining with anti-FIV p26 antibody showed that uninfected CrFK cells were essentially negative for p26 (no fluorescence; Fig. 3A), whereas the chronically FIV-Petaluma-infected CrFK cells showed strong p26 fluorescent staining (Fig. 3B). The morphology of the infected cells also appeared altered—smaller and rounder, with a tendency to cluster together. Treatment of FIV-infected cells with 2 μM D4E1 for 3 days diminished the cell-associated fluorescence indicative of FIV p26 (Fig. 3C). The alleviation of the cell pathological phenomena could be the consequence of reduced viral load, as assessed by p26 levels in the culture.

**Long-term suppression of infectious FIV progeny by peptidyl-MIM.** Chronically FIV-Petaluma-infected CrFK cells treated with a single 2 μM dose of peptidyl-MIM D4E1 for 7 days showed consistent reduction of extracellular FIV Gag protein p26 to 50, 57, 64, and 45% of the control value at days 1, 3, 5, and 7, respectively. A further reduction in infectious progeny virus at 7 days was detected by the $TCID_{50}$ assay. Figure 4 shows a >2-log reduction in infectious virus in D4E1-treated culture compared to controls. No infectious virus was detected prior to day 7 posttreatment (data not shown). This study indicates long-term virus suppression by D4E1, and suppression of infectious virus was more profound than reduction in p26 production.

**Peptidyl-MIMs do not affect FIV binding, entry, or mRNA levels.** Virus binding and entry were characterized based on the facts that virus binds to but cannot penetrate the cell membrane at 4°C and that trypsin treatment removes externally bound virus but has no effect on internalized virus (9, 15). CrFK cells infected with FIV-Petaluma at 4°C had significant viral *gag* RNA as detected by RT-PCR, whereas trypsin clearly reduced this band (Fig. 5A). In contrast, when cells were infected at 37°C, FIV *gag* RNA was detected from both trypsin-treated and untreated cells.

To quantify the percentage of virus removed by trypsin treatment at 4°C, RT-qcPCR was performed. The results are shown as the *gag*/G3PDH ratio (Fig. 5B) and confirmed that greater than 90% of the cell surface-bound FIV had been removed. As shown in Fig. 6, RNA from uninfected cells had a G3PDH

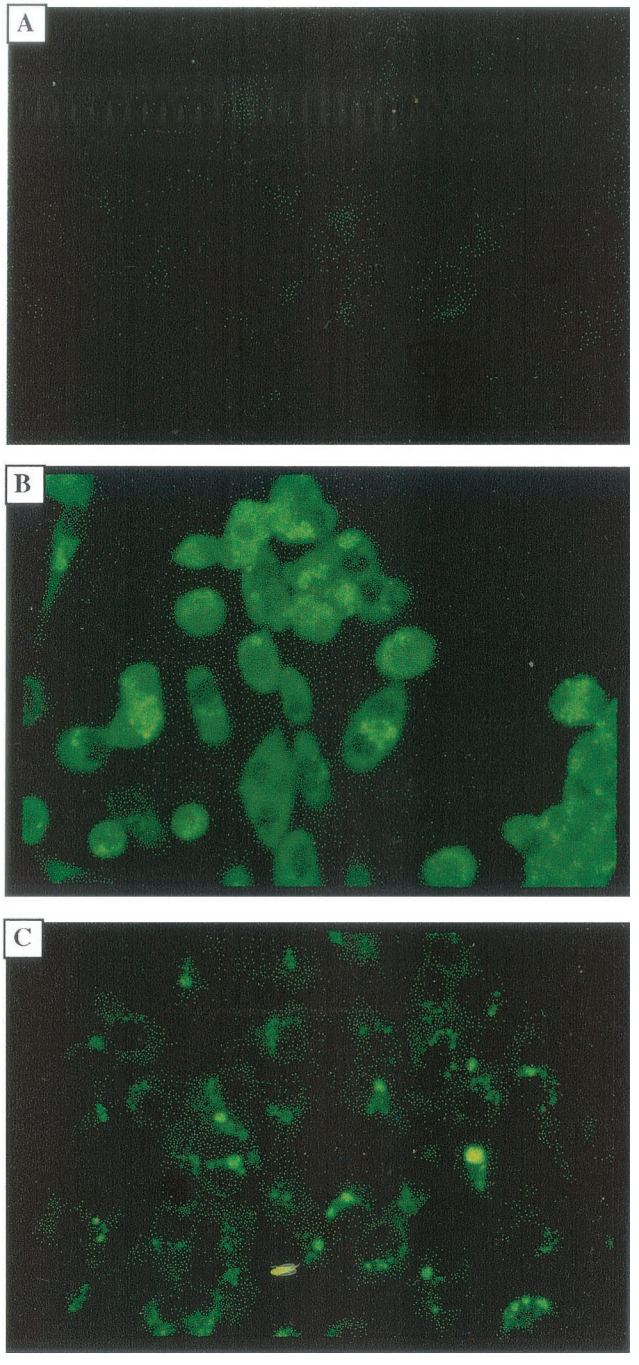


FIG. 3. Peptidyl-MIM D4E1 reduced intracellular p26 protein in FIV-infected CrFK cells. Uninfected and chronically FIV-Petaluma-infected CrFK cells were cultured on glass chamber slides with or without 2 μM D4E1 for 3 days, then stained with monoclonal antibody specific for FIV p26, followed by fluorescein-conjugated anti-mouse IgG antibody, and cells were evaluated under an epifluorescent microscope. Magnification, ×400. (A) Uninfected CrFK cells. (B) Infected untreated CrFK cells. (C) Infected D4E1-treated CrFK cells.

band (internal control), but the *gag* band was absent (lane 2). Both D4E1-treated (lane 5 and 6) and untreated (lane 3 and 4) virus-infected cells had *gag* bands amplified, and there was no reduction in the density of the band in the D4E1-treated samples. In contrast, RNA from virus only had a strong band at the position of *gag* and showed only a slightly faint band at the position of the housekeeping gene G3PDH (lane 7). These results indicate the specificity of the PCR for G3PDH and *gag* and that D4E1 does not prevent FIV binding to the cells.

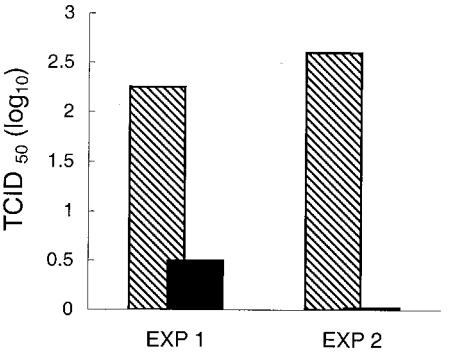


FIG. 4. Supernatants from a D4E1-treated chronically infected culture have low infectivity compared to those from the untreated culture. Chronically FIV-Petaluma-infected CrFK cells were treated with a single dose of 2 μM D4E1 peptidyl-MIM and cultured for 7 days. Supernatant collected at day 7 was tested for $TCID_{50}$ as described in Materials and Methods. Two separate experiments are shown. Striped bars, untreated supernatant; solid black bars, D4E1-treated supernatant. The results show a significant reduction in infectivity in the D4E1-treated culture.

CrFK cells were infected with FIV-Petaluma at 37°C with or without D4E1 and then treated with trypsin. Cells infected at 37°C followed by trypsin treatment produced an RT-PCR-amplified *gag* band in both D4E1-treated and untreated cells (data not shown), suggesting that D4E1 treatment does not significantly inhibit FIV penetration into CrFK cells.

Chronically infected CrFK cells incubated with or without D4E1 for 24 h were extracted for total cellular RNAs. RT-qcPCR analysis revealed mean *gag*/G3PDH ratios of 0.18 ± 0.086 for untreated cells, compared to 0.22 ± 0.095 for D4E1-treated cells, which is statistically insignificant ($P = 0.83$). These results suggest that D4E1 has no effect on virus mRNA production.

**Effect of peptidyl-MIM on FIV protein synthesis and virus release.** Supernatant and cells from chronically infected or uninfected CrFK cells were treated with or without 2 μM D4E1 for 24 h and assayed for virus particle proteins by SDS-PAGE and Western blotting with FIV-positive antiserum. Figure 7 shows a representative result of three independent experiments. Samples from uninfected cells did not react with FIV-positive serum (lanes 1, 2, 5, and 6). In chronically infected CrFK cells, five FIV-positive bands appeared in cell-associated samples (lane 3 and 4) having molecular weights corresponding approximately to those of Gag/Pol p145, Gag p55, envelope protein gp40, and mature Gag products p26 (capsid protein) and p15 (matrix protein).

D4E1 treatment did not affect FIV protein synthesis, as demonstrated by the presence of similar levels of p145 and p55 precursor proteins in untreated (lane 3) and treated (lane 4) cells. However, the mature p26 product and, to a lesser extent, p40 and p15 increased in D4E1-treated cells (lane 4) compared to untreated cells (lane 3), indicating that the virus budding process may be blocked. In the extracellular supernatant sam-

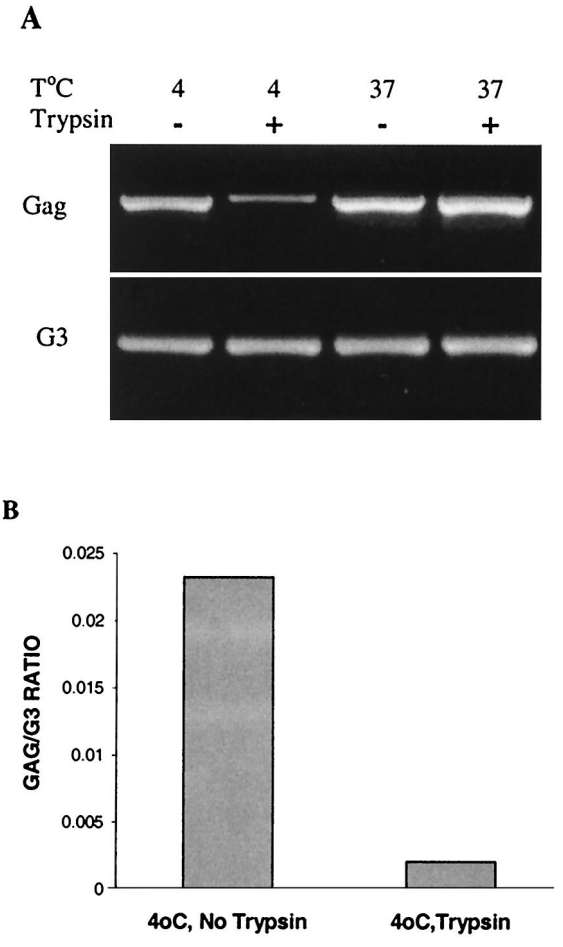


FIG. 5. Differentiation of cell-associated external and internal virus. CrFK cells were infected with FIV-Petaluma at 4 or 37°C, followed by trypsin to discriminate between bound (external) and internalized virus. (A) RT-PCR was performed with primers specific for FIV *gag* and G3PDH (internal control). Trypsin treatment reduced cell-associated *gag* RNA to minimal levels when viral infection was performed at 4°C but not at 37°C. (B) RT-qcPCR was performed with primers specific for *gag* and G3PDH with a competitive fragment (see diagram, Fig. 1), and the results are expressed as the *gag*:G3PDH (G3) ratio. Trypsin treatment reduced cell-associated *gag* RNA to less than 10% of that found in the untreated culture when viral infection was performed at 4°C.

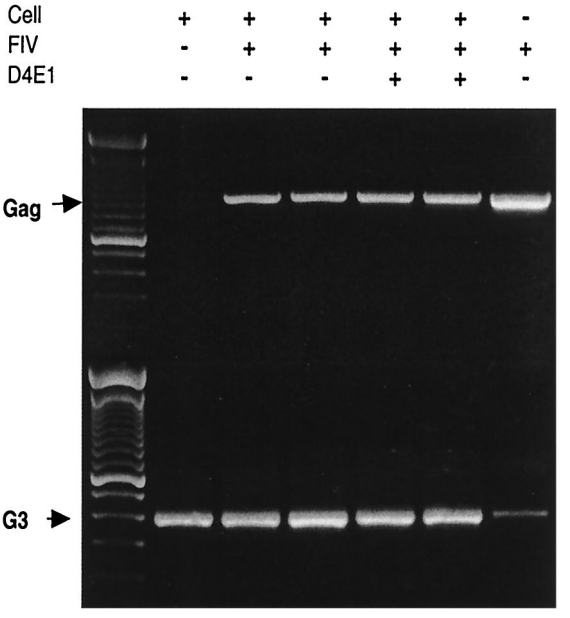


FIG. 6. Effect of peptidyl-MIM D4E1 treatment on FIV binding. CrFK cells were infected with FIV-Petaluma at 4°C with or without 2 μM D4E1 treatment; cell-associated viral RNA was extracted and amplified by RT-PCR for *gag* and G3PDH. From left: lane 2, cells only; lanes 3 and 4, duplicate cultures without D4E1; lanes 5 and 6, duplicate cultures with D4E1 treatment; lane 7, virus only.

ples, two FIV-positive bands appeared which corresponded to p26 and p15. D4E1 treatment significantly decreased these two proteins (lane 8) compared to levels in untreated cell culture supernatants (lane 7). Taken together, the equal levels of precursor protein Gag p55 in the cells, the enhanced intracellular mature Gag product p26, and the decreased extracellular p26 in D4E1-treated FIV-infected CrFK cells suggest that D4E1 may block FIV particle budding out or release from the cell membrane.

**Noninfectious virus produced from peptidyl-MIM-treated cultures can bind to and enter cells.** The previous experiment showed that infectious virus was reduced approximately 2 logs after a single treatment with D4E1 (Fig. 4) To determine if the virions produced from D4E1-treated cultures were capable of infecting CrFK cells, cells were infected by virions from D4E1-treated and untreated cultures for 3 days, and DNA was purified and analyzed by nested PCR. The quantity of virus used to infect cells was either 100 or 45 μl (based on normalization from p26 expression). As shown in Fig. 8, lanes 7 to 10, nested PCR amplification detected proviral DNA in as few as $10^3$ cells in the culture infected with virions from the untreated culture, while proviral DNA was only detected in $10^5$ cells of the D4E1-treated culture (lanes 11 to 14). This indicates that the virions produced from D4E1-treated cells are mostly noninfectious.

We further asked whether these defective virions were capable of binding to and entering the cell. The results (Fig. 9) showed that binding was comparable between virus derived from untreated (lane 5) and D4E1-treated (lane 6) cells. Similarly, virus internalization was comparable between untreated (lane 10) and D4E1-treated (lane 11) cells. RT-PCR of viral RNA from D4E1-treated and untreated culture supernatants also confirmed the ELISA results (45% of the control), as the band in lane 12 (untreated) had twice the intensity of that in lane 13 (D4E1 treated).

These results indicate that D4E1 reduced virus production. Reduction in infectious virus was more marked than reduction in p26 production, suggesting that D4E1 may affect some post-translation step, such as virus assembly or release.

## DISCUSSION

A number of natural peptide antibiotics and their synthetic peptidyl analogs have been shown to have a broad range of antimicrobial activity (4, 16). Although many studies have reported the antibacterial, antifungal, and antiprotozoal activities of these peptides, only a few studies have evaluated the

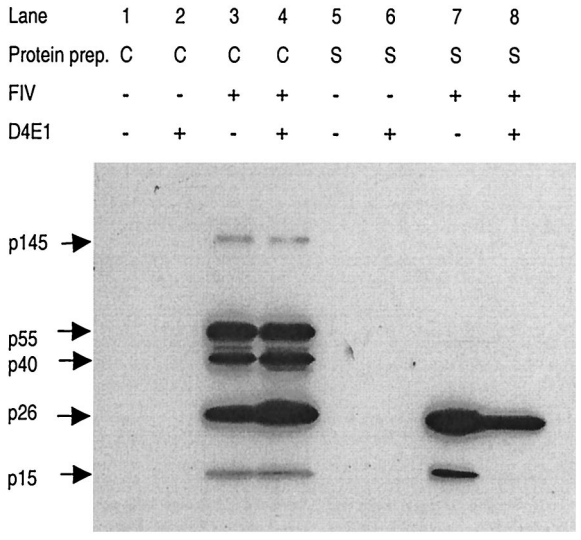


FIG. 7. Western blot analysis of effects of D4E1 on FIV protein synthesis and virus release. Uninfected and chronically infected CrFK cells were cultured with or without 2 μM D4E1 for 24 h, and cell or supernatant samples were resolved by SDS-PAGE and immunodetected with FIV-positive serum. Lanes 1-4: cell-associated proteins (C, intracellular proteins); lanes 5-8: supernatant-associated proteins (S, extracellular proteins). Samples prepared from infected and uninfected cells with or without D4E1 treatments are as indicated in the figure. Five visible bands were seen in the cell-associated protein preparation from FIV-infected culture (lanes 3 and 4), which correspond to viral proteins Gag/pol p145, Gag p55, gp40, Gag p26, and Gag p15. Two bands (Gag p26 and p15) were detected in the supernatants. The results show an equivalent amount of p145 and p55, enhanced cell-associated p26, and decreased supernatant-associated p26. The result shown here was representative of three independent experiments.

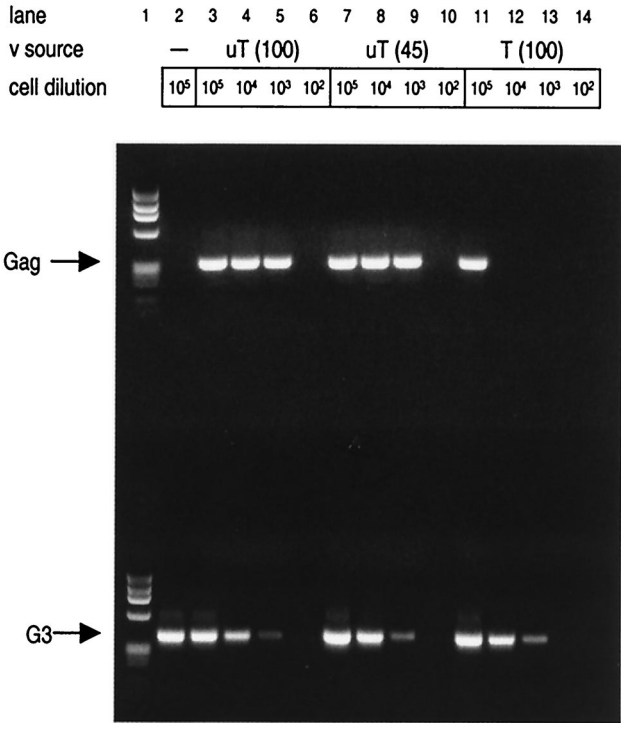


FIG. 8. FIV produced from D4E1-treated cultures is mostly noninfectious. Chronically FIV-Petaluma-infected CrFK cells were treated with a single dose of 2 μM D4E1 peptidyl-MIM and cultured for 7 days. The supernatant collected was added to a monolayer of CrFK cells for 3 days. Infectivity was analyzed by limiting-dilution nested PCR for proviral DNA. The infection conditions and cell dilutions are indicated at the top of the figure. The quantity of virus used to infect cells was either 100 or 45 μl (based on normalization from p26 expression) of day 7 culture supernatant. uT, virus from the untreated culture; T, virus from the D4E1-treated culture. Proviral DNA was amplified only in $10^5$ cells from D4E1-treated virus cultures [T(100)] compared to as few as $10^3$ in untreated infected cultures [uT(45)], suggesting that the virions produced by the D4E1-treated culture were mostly noninfectious.

antiviral activity and characterized the mechanisms of action (28, 45, 46). In this study, a panel of synthetic peptidyl-MIMs were tested for antiretroviral activity against FIV-infected CrFK cells. These peptidyl-MIMs were designed to enhance their antimicrobial activities while retaining low host cell toxicity; the conserved α-helix and β-sheet motifs of natural peptide antibiotics were modified in length, charge, and hydrophobicity. Three of 16 peptidyl-MIM candidates, D4E1, DC1, and D1D6, effectively inhibited FIV RT activity, with $IC_{50}$ values of 0.46 to 0.94 μM, which were 10 times lower than the $TC_{50}$. The in vitro (inferred) therapeutic indices were 12.8, 12.3, and 9.5, respectively, for these potent candidates, suggesting potential as novel antiretroviral agents. The experiments also showed effective reduction of infectious virus progeny in the cell culture supernatant, alleviation of cell pathological phenomena, and reduction of the intracellular virus burden.

Similar results were obtained by Wachinger et al. (45, 46), who showed that the peptide antibiotics melittin, cecropin, and their derivatives inhibited replication of two strains of HIV in vitro. They obtained $IC_{50}$ values of 0.4 to 2 μM, which were very similar to those found in the present study, and these concentrations also were not cytotoxic. In view of these similarities, the results may reflect general antiretroviral activity for antimicrobial peptides.

Studies on the direct effects of peptidyl-MIM D4E1 on several key steps of the FIV replication cycle were carried out. FIV binding was not affected by D4E1 treatment, as indicated by the similar levels of amplification of cell-associated virus *gag* RNA when the cells were infected at 4°C. Similarly, D4E1 treatments had no significant effect on virus internalization at 37°C or on virus transcription. However, analysis of cell-associated and virus-associated viral proteins by Western blot revealed an intracellular accumulation of mature Gag protein p26 and reduced extracellular Gag p26. This accumulation of mature Gag p26 was not due to the increase in viral protein synthesis, as the Gag precursor (p145 and p55) levels were similar in the untreated and D4E1-treated cells. Mature p26 is a product of the Gag polyprotein which is cleaved by viral protease. Protease is activated after the dimerization of two Gag-Pol fusion proteins, which happens during or shortly after assembly (34). The accumulation of the p26 protein within the cell indicates that D4E1 inhibits virus production during or after virus assembly and before virus budding from the cell membrane.

Experiments to characterize FIV protein p26 expression in chronically infected CrFK cells were conducted under different conditions. Changes in p26 were associated with treatment of chronically infected cells with peptidyl-MIM D4E1. However,

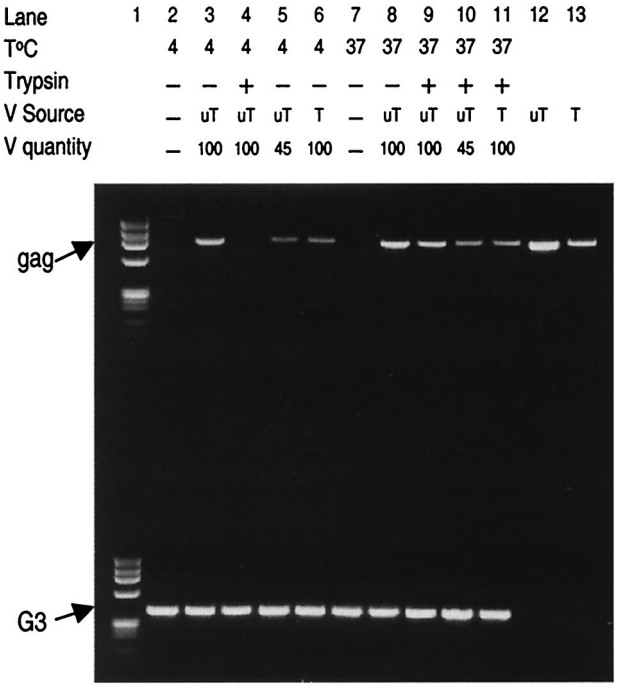


FIG. 9. FIV produced from D4E1-treated cells binds to and enters CrFK cells. Chronically FIV-Petaluma-infected CrFK cells were treated with a single dose of 2 μM D4E1 peptidyl-MIM and cultured for 7 days. Virus produced was analyzed for the ability to bind to and enter CrFK cells. Treatment conditions are indicated at the top of the figure and are also described in the legend to Fig. 5 and in Materials and Methods. The quantity of virus used to infect cells was either 100 or 45 μl (based on normalization from p26 expression) of day 7 culture supernatant. uT, virus from the untreated culture; T, virus from the D4E1-treated culture. No difference in the abilities of untreated and treated virus supernatants to bind (lane 5 and 6) and internalize (lane 10 and 11) was seen. Direct RT-PCR of viral supernatant from untreated (lane 12) and treated (lane 13) cultures is shown. This experiment indicates that virus produced from D4E1-treated cells is able to bind to and internalize in CrFK cells.

short-term treatment with D4E1 may induce a transient increase in cell-associated p26 while decreasing the amount of p26 in culture supernatants (as shown in Fig. 8). Longer exposures (3 days) in continuous culture with D4E1 may be required to inhibit intracellular FIV p26 as detectable by immunocytofluorescence (Fig. 3). In addition, other factors such as outgrowth of uninfected cells may contribute to these changes.

An interesting observation from this study is that peptidyl-MIM appears to have a more pronounced inhibitory effect on the production of infectious virus than on the production of p26 viral proteins in chronically infected cells. This prompted us to further investigate whether virions produced from D4E1-treated cells were able to bind to, enter, and replicate in CrFK cells. Our results indicate that these viruses are normal in binding and internalization (Fig. 9) but have decreased ability to produce infectious virus compared to virus from untreated cells (Fig. 8).

Membranes have long been recognized as targets for many peptide antibiotics, having α-helix and/or β-sheet secondary structures and amphipathic and cationic characters (19, 20, 40). The membrane-targeted activity of peptide antibiotics was demonstrated in voltage-dependent channel formation in artificial membranes (1, 18), lysis of liposomes, and direct lysis of enveloped virus (2, 8, 11, 21, 27, 43). Despite general membrane disruption phenomena, the peptide antibiotics generally have strong selectivity against microbes but not normal host cells. The basis for the selectivity is considered to be the differences in size of the transmembrane electrical potential gradient and the lipid composition of the membranes of bacterial and host cells. However, as the envelope of the virus actually originates from the host cell membrane, both membranes have similar lipid compositions. Nonetheless, the concentration of peptide antibiotics inhibiting virus production from host cells usually is much lower than the virolytic concentration, suggesting more complex mechanisms instead of direct penetration of the membrane (46).

The unique secondary structure (α-helix and β-pleated sheets) of synthetic and natural peptide antibiotics may interact with either host or viral proteins via charge, hydrophobicity, amphipathicity, or spatial chiral structure to inhibit protein function important for viral replication. For example, T22 (a peptide modeled after polyphemusin isolated from the hemocytes of horseshoe crabs) inhibited HIV fusion by binding to CXCR4, a chemokine receptor that serves as a coreceptor for the entry of T-cytotropic HIV-1 strains (28). A second example is melittin and one of its synthetic peptide analogs, which inhibit the infectivity of the tobacco mosaic virus by perturbing its assembly due to the similarity of melittin to a virus capsid region involved in RNA interaction (23). Peptides consisting of sequences taken from viral proteins or having secondary structure (amphipathic α-helix or β-pleated sheet) similar to those of viral protein have been shown to impair viral infectivity (6, 33, 47). These reports suggest that the similarity of peptide antibiotics in both sequence and secondary structure to viral proteins may be essential to the mechanism of their antiviral activity.

The results from our experiments seem to favor this hypothesis. Stepwise identification of the inhibition of viral replication by D4E1 indicates that virus production was blocked at assembly and release rather than a general membrane disruption. Prior to virus assembly, the N-terminal glycine of the P17 MA domain of Gag or Gag-Pol protein is myristylated to direct the Gag protein to the host cell membrane and anchor envelope protein to the virion capsid (5). The amphipathic β-sheet structure of D4E1 could interrupt this connection by binding to the Env gp41 transmembrane protein, which also has a strong amphipathic segment in the carboxyl terminus (24), as has been suggested for defensins (having an amphipathic β-sheet structure similar to that of D4E1 [25]) and magainin-2 (24).

The present data demonstrate that the amphipathic β-sheet structure of peptidyl-MIM D4E1 may facilitate interference with viral assembly or release and reduce the number of infectious progeny virions. This activity represents an effective antiviral strategy with a potentially wide therapeutic window. These results should encourage the further study of synthetic peptide membrane-interactive molecules for use as therapeutic agents.

## ACKNOWLEDGMENTS

This work was supported by Demegen Inc., Pittsburgh, Pa.

We thank Barry P. Peter and Scott M. Laster for valuable discussions and technical expertise and appreciate the technical assistance of Tedd A. Childers, Joseph G. Bucci, Lori Scappino, and Lise Barley-Maloney. We also acknowledge Mindy Reese for review of the manuscript during its preparation.

## REFERENCES


1. **Agawa, Y., S. Lee, S. Ono, H. Aoyagi, M. Ohno, T. Taniguchi, K. Anzai, and Y. Kirino.** 1991. Interaction with phospholipid bilayers, ion channel formation, and antimicrobial activity of basic amphipathic alpha-helical model peptides of various chain lengths. J. Biol. Chem. **266:**20218–20222.
2. **Baghian, A., J. Jaynes, F. Enright, and K. G. Kousoulas.** 1997. An amphipathic alpha-helical synthetic peptide analogue of melittin inhibits herpes simplex virus-1 (HSV-1)-induced cell fusion and virus spread. Peptides **18:** 177–183.
3. **Boman, H.** 1995. Peptide antibiotics and their role in innate immunity. Annu. Rev. Immunol. **13:**61–92.
4. **Boman, H. G.** 1994. Antimicrobial peptides. Chairman's opening remarks. CIBA Found. Symp. **186:**1–4.
5. **Bryant, M., and L. Ratner.** 1990. Myristoylation-dependent replication and assembly of human immunodeficiency virus 1. Proc. Natl. Acad. Sci. USA **87:**523–527.
6. **Chen, C. H., T. J. Matthews, C. B. McDanal, D. P. Bolognesi, and M. L. Greenberg.** 1995. A molecular clasp in the human immunodeficiency virus (HIV) type 1 TM protein determines the anti-HIV activity of gp41 derivatives: implication for viral fusion. J. Virol. **69:**3771–3777.
7. **Cohen, J.** 1997. The daunting challenge of keeping HIV suppressed. Science **277:**32–33.
8. **Daher, K. A., M. E. Selsted, and R. I. Lehrer.** 1986. Direct inactivation of viruses by human granulocyte defensins. J. Virol. **60:**1068–1074.
9. **de Parseval, A., D. L. Lerner, P. Borrow, B. J. Willett, and J. H. Elder.** 1997. Blocking of feline immunodeficiency virus infection by a monoclonal antibody to CD9 is via inhibition of virus release rather than interference with receptor binding. J. Virol. **71:**5742–5749.
10. **English, R. V., P. Nelson, C. M. Johnson, M. Nasisse, W. A. Tompkins, and M. B. Tompkins.** 1994. Development of clinical disease in cats experimentally infected with feline immunodeficiency virus. J. Infect. Dis. **170:**543–552.
11. **Esser, A. F., R. M. Bartholomew, F. C. Jensen, and H. J. Muller-Eberhard.** 1979. Disassembly of viral membranes by complement independent of channel formation. Proc. Natl. Acad. Sci. USA **76:**5843–5847.
12. **Hancock, R. E.** 1999. Host defence (cationic) peptides: what is their future clinical potential? Drugs **57:**469–473.
13. **Hancock, R. E., and R. Lehrer.** 1998. Cationic peptides: a new source of antibiotics. Trends Biotechnol. **16:**82–88.
14. **Hawkes, R.** 1979. General principles underlying laboratory diagnosis of viral infection, p. 32–35. *In* E. Lennette and R. Schmidt (ed.), Diagnostic procedures for viral, rickettsial, and chlamydial infections, 5th ed. American Public Health Association, Inc., Washington, D.C.
15. **Herbein, G., L. J. Montaner, and S. Gordon.** 1996. Tumor necrosis factor alpha inhibits entry of human immunodeficiency virus type 1 into primary human macrophages: a selective role for the 75-kilodalton receptor. J. Virol. **70:**7388–7397. (Erratum, **71:**1581, 1997.)
16. **Jaynes, J.** 1990. Lytic peptides portend an innovative age in the management and treatment of human disease. Drug News Perspect. **3:**69–78.
17. **Johnson, D., J. Gautsch, R. Sportsman, and J. Elder.** 1983. Improved technique utilizing non-fat dry milk for analysis of protein and nucleic acids transferred to nitrocellulose. Gene Anal. Technol. **1:**3–7.
18. **Kagan, B. L., M. E. Selsted, T. Ganz, and R. I. Lehrer.** 1990. Antimicrobial defensin peptides form voltage-dependent ion-permeable channels in planar lipid bilayer membranes. Proc. Natl. Acad. Sci. USA **87:**210–214.
19. **Lehrer, R. I., A. Barton, K. A. Daher, S. S. Harwig, T. Ganz, and M. E. Selsted.** 1989. Interaction of human defensins with *Escherichia coli*. Mechanism of bactericidal activity. J. Clin. Investig. **84:**553–561.
20. **Lehrer, R. I., A. Barton, and T. Ganz.** 1988. Concurrent assessment of inner and outer membrane permeabilization and bacteriolysis in *E. coli* by multiple-wavelength spectrophotometry. J. Immunol. Methods **108:**153–158.
21. **Lehrer, R. I., K. Daher, T. Ganz, and M. E. Selsted.** 1985. Direct inactivation of viruses by MCP-1 and MCP-2, natural peptide antibiotics from rabbit leukocytes. J. Virol. **54:**467–472.
22. **Ma, J., S. Kennedy-Stoskopf, R. Sellon, S. Tonkonogy, E. C. Hawkins, M. B. Tompkins, and W. A. Tompkins.** 1995. Tumor necrosis factor-alpha responses are depressed and interleukin-6 responses unaltered in feline immunodeficiency virus infected cats. Vet. Immunol. Immunopathol. **46:**35–50.
23. **Marcos, J. F., R. N. Beachy, R. A. Houghten, S. E. Blondelle, and E. Perez-Paya.** 1995. Inhibition of a plant virus infection by analogs of melittin. Proc. Natl. Acad. Sci. USA **92:**12466–12469.
24. **Miller, M. A., R. F. Garry, J. M. Jaynes, and R. C. Montelaro.** 1991. A structural correlation between lentivirus transmembrane proteins and natural cytolytic peptides. AIDS Res. Hum. Retrovir. **7:**511–519.
25. **Monell, C. R., and M. Strand.** 1994. Structural and functional similarities between synthetic HIV gp41 peptides and defensins. Clin. Immunol. Immunopathol. **71:**315–324.
26. **Mosmann, T.** 1983. Rapid colorimetric assay for cellular growth and survival: application to proliferation and cytotoxicity assays. J. Immunol. Methods **65:**55–63.
27. **Murakami, T., M. Niwa, F. Tokunaga, T. Miyata, and S. Iwanaga.** 1991. Direct virus inactivation of tachyplesin I and its isopeptides from horseshoe crab hemocytes. Chemotherapy **37:**327–334.
28. **Murakami, T., T. Y. Zhang, Y. Koyanagi, Y. Tanaka, J. Kim, Y. Suzuki, S. Minoguchi, H. Tamamura, M. Waki, A. Matsumoto, N. Fujii, H. Shida, J. A. Hoxie, S. C. Peiper, and N. Yamamoto.** 1999. Inhibitory mechanism of the CXCR4 antagonist T22 against human immunodeficiency virus type 1 infection. J. Virol. **73:**7489–7496.
29. **Nakashima, H., M. Masuda, T. Murakami, Y. Koyanagi, A. Matsumoto, N. Fujii, and N. Yamamoto.** 1992. Anti-human immunodeficiency virus activity of a novel synthetic peptide, T22 ([Tyr-5,12, Lys-7]polyphemusin II): a possible inhibitor of virus-cell fusion. Antimicrob. Agents Chemother. **36:**1249–1255.
30. **North, T. W., G. L. North, and N. C. Pedersen.** 1989. Feline immunodeficiency virus, a model for reverse transcriptase-targeted chemotherapy for acquired immune deficiency syndrome. Antimicrob. Agents Chemother. **33:** 915–919.
31. **Novotney, C., R. V. English, J. Housman, M. G. Davidson, M. P. Nasisse, C. R. Jeng, W. C. Davis, and M. B. Tompkins.** 1990. Lymphocyte population changes in cats naturally infected with feline immunodeficiency virus. AIDS **4:**1213–1218.
32. **Oren, Z., and Y. Shai.** 1998. Mode of action of linear amphipathic alpha-helical antimicrobial peptides. Biopolymers **47:**451–463.
33. **Owens, R. J., C. C. Tanner, M. J. Mulligan, R. V. Srinivas, and R. W. Compans.** 1990. Oligopeptide inhibitors of HIV-induced syncytium formation. AIDS Res. Hum. Retrovir. **6:**1289–1296.
34. **Pavlakis, G.** 1997. The molecular biology of human immunodeficiency virus type 1, p. 45–74. *In* V. De Vita, Jr., S. Hellman, and S. Rosenberg (ed.), AIDS: biology, diagnosis, treatment and prevention, 4th ed. Raven-Lippincott, Philadelphia, Pa.
35. **Pedersen, N. C., J. K. Yamamoto, T. Ishida, and H. Hansen.** 1989. Feline immunodeficiency virus infection. Vet. Immunol. Immunopathol. **21:**111–129.
36. **Roberts, N. A.** 1995. Drug-resistance patterns of saquinavir and other HIV proteinase inhibitors. AIDS **9**(Suppl. 2)**:S**27–S32.
37. **Rogers, A.** 1998. Maternal-fetal feline immunodeficiency virus transmission: timing and tissue tropisms. J. Infect. Dis. **178:**960–967.
38. **Rottman, J. B., W. A. Tompkins, and M. B. Tompkins.** 1996. A reverse transcription-quantitative competitive polymerase chain reaction (RT-qcPCR) technique to measure cytokine gene expression in domestic mammals. Vet. Pathol. **33:**242–248.
39. **Smyth, N. R., C. McCracken, R. M. Gaskell, J. M. Cameron, J. A. Coates, C. J. Gaskell, C. A. Hart, and M. Bennett.** 1994. Susceptibility in cell culture of feline immunodeficiency virus to eighteen antiviral agents. J. Antimicrob. Chemother. **34:**589–594.
40. **Steiner, H.** 1982. Secondary structure of the cecropins; antibacterial peptides from the moth *Hyalophora cecropia*. FEBS Lett. **137:**283–287.
41. **Talbott, R. L., E. E. Sparger, K. M. Lovelace, W. M. Fitch, N. C. Pedersen, P. A. Luciw, and J. H. Elder.** 1989. Nucleotide sequence and genomic organization of feline immunodeficiency virus. Proc. Natl. Acad. Sci. USA **86:**5743–5747.
42. **Tam, J., C. Wu, and J. Yang.** 2000. Membranolytic selectivity of cystine-stabilized cyclic protegrins. Eur. J. Biochem. **267:**3289–3300.
43. **Tamamura, H., T. Murakami, M. Masuda, A. Otaka, W. Takada, T. Ibuka, H. Nakashima, M. Waki, A. Matsumoto, N. Yamamoto, et al.** 1994. Structure-activity relationships of an anti-HIV peptide T22. Biochem. Biophys. Res. Commun. **205:**1729–1735.
44. **Tompkins, M. B., P. D. Nelson, R. V. English, and C. Novotney.** 1991. Early events in the immunopathogenesis of feline retrovirus infections. J. Am. Vet. Med. Assoc. **199:**1311–1315.
45. **Wachinger, M., A. Kleinschmidt, D. Winder, N. von Pechmann, A. Ludvigsen, M. Neumann, R. Holle, B. Salmons, V. Erfle, and R. Brack-Werner.** 1998. Antimicrobial peptides melittin and cecropin inhibit replication of human immunodeficiency virus 1 by suppressing viral gene expression. J. Gen. Virol. **79:**731–740.
46. **Wachinger, M., T. Saermark, and V. Erfle.** 1992. Influence of amphipathic peptides on the HIV-1 production in persistently infected T lymphoma cells. FEBS Lett. **309:**235–241.
47. **Wild, C., T. Oas, C. McDanal, D. Bolognesi, and T. Matthews.** 1992. A synthetic peptide inhibitor of human immunodeficiency virus replication: correlation between solution structure and viral inhibition. Proc. Natl. Acad. Sci. USA **89:**10537–10541.